

# Influence of Static and Dynamic Disorder on the Anisotropy of Emission in the Ring Antenna Subunits of Purple Bacteria Photosynthetic Systems

**Pavel Heřman**

*Department of Physics, University of Hradec Králové, V. Nejedlého 573,  
CZ-50003 Hradec Králové, Czech Republic  
e-mail: pavel.herman@uhk.cz*

**Ulrich Kleinekathöfer**

*Institut für Physik, Technische Universität, D-09107 Chemnitz, Germany  
e-mail: kleinekathoefer@physik.tu-chemnitz.de*

**Ivan Barvák**

*Institute of Physics, Charles University, Ke Karlovu 5,  
CZ-12116 Prague, Czech Republic  
e-mail: barvik@karlov.mff.cuni.cz*

**Michael Schreiber**

*Institut für Physik, Technische Universität, D-09107 Chemnitz, Germany  
e-mail: schreiber@physik.tu-chemnitz.de*

## Abstract

Using the reduced density matrix formalism the time dependence of the exciton scattering in light-harvesting ring systems of purple bacteria is calculated. In contrast to the work of Kumble and Hochstrasser (J. Chem. Phys. 109 (1998) 855) static disorder (fluctuations of the site energies) as well as dynamic disorder (dissipation) is taken into account. For the description of dissipation we use Redfield theory in exciton eigenstates without secular approximation. This is shown to be equivalent to the Markovian limit of Čápek's theory in local states. Circular aggregates with 18 pigments are studied to model the B850 ring of bacteriochlorophylls within LH2 complexes. It can be demonstrated that the dissipation is important for the time-dependent anisotropy of the fluorescence. Smaller values of static disorder are sufficient to produce the same decay rates in the anisotropy in comparison with the results by Kumble and Hochstrasser.

# 1 Introduction

The physical motivation of the present paper is a growing interest in the exciton transfer in the antenna systems (ASs) of the purple bacteria photosynthetic units (PSUs). The light-harvesting complexes that are present in photosynthetic systems perform two major functions: harvest (absorb) the incident light and transport the energy in form of Frenkel excitons to the reaction center (RC). Many investigations, both experimental and theoretical ones, have been directed towards understanding of the exciton transfer in the ASs of purple bacteria PSUs and are reviewed in [1–3, and references therein]. Although considerable progress has been made during recent years, our knowledge about the mechanism of energy transfer and relaxation is still far from complete.

In 1995 the first high-resolution three-dimensional X-ray structure of a bacterial antenna complex LH2 from *Rhodospseudomonas acidophila* was published by Mc Dermott et al. [4,5]. It consists (see Fig. 2 in [5]) of nine identical units, protomers, each of which is formed by two proteins ( $\alpha$  and  $\beta$ ) with bound bacteriochlorophylls (BChl). The nine  $\alpha$  subunits are packed in an inner ring to form a hollow cylinder of radius 1.8 nm. The 9  $\beta$  subunits are arranged radially outwards with respect to the  $\alpha$  subunits to form another ring with a radius of 3.4 nm. The protein serves as a scaffold for the BChls and furthermore specifically influences the spectroscopic properties of the BChls by supplying a characteristic environment for them. A ring with a radius of about 2.5 nm of 18 BChl molecules is sandwiched between the  $\alpha$  and  $\beta$  subunits.

The very symmetric arrangement with short distances between the pigments provides a new impulse to the discussion about, e.g., the exciton transfer regime and the exciton delocalization in LH2. The extent of the exciton delocalization, which could be reduced by dynamic and static disorders, has been discussed. The principal question reads: Are the states contributing to the optical and transport properties of the LH2 ring localized or delocalized?

In the past knowledge of the energy transfer was mainly derived from steady state spectroscopic experiments leading to several absorption bands at different wavelengths. Pigment molecules B850, that we are dealing with, are characterized by the absorption wavelength in the LH2 subunits of the ASs of purple bacteria. At room temperature the solvent and the protein environment fluctuate with characteristic time scales ranging from femtoseconds to nanoseconds. The dynamical aspects of the system are reflected in the line shapes of the electronic transitions. To fully characterize the line shape of a transition and thereby the dynamics of the system, one needs to know not only the fluctuation amplitude  $\Delta$  (coupling strength) but also the time scale of each process involved. The observed linewidths reflect the combined influence of static disorder and exciton coupling to intermolecular, intramolecular, and solvent nuclear motions. The simplest approach is to decompose the line profile into homogeneous and inhomogeneous contributions. In more sophisticated models, each process is defined with its characteristic time scale as well as a coupling strength [6–9].

Both the exciton-phonon coupling and the static disorder lead to localization of excitons. One tries to avoid the influence either of the dynamical disorder by measuring at very low temperatures or of the static disorder by performing single-molecule spectroscopy experiments. The absorption, circular dichroism, and hole-burning spectra of the LH2 complex are reproduced reasonably well by theoretical treatments, that consider Frenkel exciton states of the entire complex but invoke moderate disorder in the excitation energies of the individual BChls [1].

In a homogeneous system, in which the  $Q_y$  transition dipole moments of the B850 BChls all lie approximately in the plane of the ring, most of the dipole strength of the B850 band would come from a degenerate pair of orthogonally polarized transitions at an energy slightly higher than the transition energy of the lowest exciton state. However, energetic or structural disorder that disrupts the symmetry of the complex will make both the low-energy transition and transitions at higher energies weakly allowed.

Time-dependent experiments (absorption, fluorescence, photon echo, etc.), which used (sub-)picosecond light pulses of low energy with high repetition rate tunable through the infrared absorption bands of the various BChl pigments in a variety of bacterial ASs, made it possible to study the long-time as well as femtosecond dynamics of the energy transfer and relaxation [1, 10–14]. The nature of the rapid relaxation is of interest because it depends on how photosynthetic antenna complexes absorb and transfer energy and because it may provide an experimental window to protein dynamics on very short time scales [15].

The interpretation of time-dependent experiments on femtosecond time scale requires a theory which incorporates both dynamic disorder and different kinds of static disorder. Recently, models based on extended exciton states with moderate static disorder  $\Delta \approx J/2$  have found acceptance in the interpretation of the experiments [10–14, 16–20] in which it has been shown that the elementary dynamics occurs on a time scale of about 100 fs [15, 21–23]. For the ring of BChls in the LH2 antenna complex Kumble and Hochstrasser [24] has presented a time-domain analysis of the effects of local energy inhomogeneity upon the dynamics of optical excitations. They examined the manifestation of disorder scattering in polarized femtosecond spectroscopy and the degree to which exciton delocalization is revealed in emission and transient absorption anisotropy measurements. The time evolution of the quantum states, prepared by impulsive excitation of a statically disordered circular aggregate model for LH2 antenna complexes, have been calculated exactly quantum mechanically for varying degrees of inhomogeneity (static disorder), but without taking into account the interaction with a heat bath (dynamic disorder). For a Gaussian distribution of local energies, the dynamics of coherence loss (scattering) has been explored as a function of the ratio of the standard deviation  $\Delta$  of the distribution to the intersite interaction energy  $J$ . (Please note that Kumble and Hochstrasser used the symbol  $\sigma$  for the standard deviation in their paper [24].) It has been found, that modest degrees of disorder ( $\Delta/J \approx 0.4 - 0.8$ ) are suffi-

cient to cause scattering on a sub-100 fs time scale. The estimate of static disorder emerging from this investigation should be considered as an upper limit. By neglecting the influence of phonons, Kumble and Hochstrasser's model does not take into account the dynamic scattering effects which contribute to dephasing of the initial wave packet state and which promote thermalization of the dephased populations.

Nagarajan et al. [21] measured the changes in absorption and stimulated emission caused by excitation with 35 fs pulses centered at 875 nm. Substantial relaxation on the time scale of 10-100 fs and an anomalously large initial anisotropy of 0.7 in the bleaching and stimulated-emission signal has been observed. These results have been interpreted in the simple model of a homogeneous system in which excitations are delocalized over the whole ring. The high initial anisotropy was ascribed to coherent excitation of a degenerate pair of states with allowed transitions and the relaxations to electronic dephasing and equilibration with states at lower energies which have forbidden transitions. It has been shown in Ref. [15] that excitation of membrane-bound LH2 complexes with low-intensity femtosecond pulses causes changes in absorption and stimulated emission that initially depend on the excitation wavelength but relax to a quasi-equilibrium with a time constant of  $100 \pm 20$  fs. The signals have an apparent initial anisotropy of approximately 0.5 when the complex is excited with broadband pulses, and of 0.35-0.4 with narrower pulses. The anisotropy decays to 0.1 with a time constant of about 30 fs.

Using a density-matrix formalism Nagarajan et al. [15] have shown that the initial light-induced signals are consistent with coherent excitation of multiple exciton levels in an inhomogeneous ensemble of LH2 complexes and that the main features of the spectral relaxations and the anisotropy can be explained by electronic dephasing and thermal equilibration within the manifold of exciton levels. For one initial state three different possibilities of the form of the exciton density matrix  $\rho$  have been taken into account. Beside the full matrix description, which has been represented as a coherent superposition of the allowed "one exciton" states, the second is obtained by setting the off-diagonal terms of  $\rho$  to zero, which gives an incoherent mixture of one-exciton states with the same initial populations. Finally, in the third form the diagonal elements of  $\rho$  are replaced by the populations for a Boltzmann equilibrium at temperature  $T$  (with the off-diagonal terms zero).

Nagarajan et al. [15] have discussed several different processes which could contribute to the spectral relaxations and the rapid decay of the anisotropy. They concluded, that the main features of the spectral relaxations and the decay of anisotropy are reproduced well by a model that considers decay processes of electronic coherences within the manifold of the exciton states and the thermal equilibration among excitonic states. They have not attempted to calculate the dynamics theoretically. But the model described in [15] appears capable of rationalizing the observation that the anisotropy decay is faster than the spectral relaxation.

Moderate static disorder, which leads to electronic dephasing, causes a

large decrease in the calculated anisotropy, whereas the relaxation of the overall signal occurs mainly during thermalization, because the two most strongly allowed exciton states tend to be close together in energy and to have approximately orthogonal transition dipoles. Nagarjan et al. [15] concluded that the static inhomogeneity assumed in their LH2 model would cause the off-diagonal terms  $\rho_{ab}$  and  $\rho_{ba}$  of the density matrix to decay with a time constant of the order of 160 fs. This suggests that the more rapid dephasing indicated by the anisotropy decay ( $\tau \approx 30$  fs) is driven mainly by dynamic processes.

The aim of the present paper is to extend the investigation by Kumble and Hochstrasser [24] and also by Nagarjan et al. [15] taking into account the simultaneous influence of static and dynamic disorders on the exciton scattering after impulse excitation and on the time-dependent optical anisotropy. Different time dependent spectroscopic properties have been calculated before but within the secular approximation [25].

The remainder of this article is organized as follows: In the next section we present the model we have used. In section 3 several different theories giving the dynamical equations for the exciton density matrix are reviewed. Our results are presented in section 4 and in the last section we discuss them and draw some conclusions.

## 2 Model

### 2.1 Hamiltonian of the ideal rings

In this paper we deal with just one exciton, already created at time  $t = 0$ , on a ring interacting with a heat bath. The Hamiltonian therefore consists of three parts:

$$\begin{aligned} H^0 &= \sum_{m,n} J_{mn} a_m^\dagger a_n + \sum_q \hbar \omega_q b_q^\dagger b_q + \frac{1}{\sqrt{N}} \sum_m \sum_q G_q^m \hbar \omega_q a_m^\dagger a_m (b_q^\dagger + b_{-q}) \\ &= H_{\text{ex}}^0 + H_{\text{ph}} + H_{\text{ex-ph}}. \end{aligned} \quad (1)$$

The first term is the Hamiltonian  $H_{\text{ex}}^0$  belonging to the single exciton in the ideal ring. Operators  $a_m^\dagger$  or  $a_m$  create or annihilate an exciton at site  $m$ .  $J_{mn}$  for  $m \neq n$  is a transfer integral (also called resonance integral) between sites  $m$  and  $n$ . The diagonal elements  $J_{nn}$  are the local energies  $\epsilon_n$  at site  $n$  which could take into account, e.g., a dimerization  $\epsilon_{2n} \neq \epsilon_{2n+1}$ . The second term,  $H_{\text{ph}}$ , describes the phonons. We assume independent heat baths for each chromophore and the harmonic approximation for the phonons.  $b_q^\dagger$  and  $b_q$  denote phonon creation and annihilation operators, respectively. The last term,  $H_{\text{ex-ph}}$ , represents the interaction between the exciton and the bath. The exciton-phonon interaction is assumed to be site-diagonal and linear in the lattice displacements. The term  $G_q^m$  denotes the exciton-phonon coupling constant.

In the framework of the extended exciton states it is assumed that both intra-dimer  $J_{12}$  and inter-dimer  $J_{23}$  transfer integrals are strong enough to build exciton states spanning the whole rings. Inside one ring the pure exciton Hamiltonian  $H_{ex}^0$  (1) can be diagonalized using the wave vector representation with corresponding delocalized "Bloch" states and energies. Considering, e.g., only nearest neighbor transfer matrix elements  $J_{mn} = -J(\delta_{m,n+1} + \delta_{m,n-1})$ , the same local energies  $\epsilon_n$  at every site and using Fourier transformed excitonic operators (Bloch representation)

$$a_k = \sum_n a_n e^{ikn} \quad , \quad k = \frac{2\pi}{N} l \quad , \quad l = 0, \pm 1, \dots \pm N/2 \quad (2)$$

the simplest exciton Hamiltonian in  $\vec{k}$  representation reads

$$H_{ex}^0 = \sum_k E_k a_k^+ a_k \quad . \quad (3)$$

The dispersion of the excitonic energies is given by

$$E_k = -2 J \cos k \quad . \quad (4)$$

A splitting of the local degenerate exciton energies in one ring, to a band of energies  $E_k$ , corresponding to the exciton eigenstates, is produced.

## 2.2 Hamiltonian of the static disorder

The quasistatic disorder is described by the time-dependent part of the Hamiltonian  $H = H^0 + H_1(t)$ . This part

$$H_1(t) = \sum_n \epsilon_n(t) a_n^+ a_n \quad (5)$$

describes fluctuations of the local excitation energies  $\epsilon_n(t)$  due to slow motion of the protein environment. Fluctuations of the local excitation energies  $\epsilon_n(t)$  have exponentially decaying correlation functions. The mean values and correlation functions are given by

$$\begin{aligned} \langle \epsilon_n(t) \rangle &= 0, \\ \langle \epsilon_n(t) \epsilon_m(\tau) \rangle &= \delta_{mn} \Delta^2 \exp(-\lambda(t - \tau)). \end{aligned} \quad (6)$$

In what follows the simplification is used, that we work only with pure static disorder,  $\lim \lambda \rightarrow 0$ , and a Gaussian distribution for the uncorrelated local energy fluctuations  $\epsilon_n^s$  with a standard deviation  $\Delta$ .

## 2.3 Microscopic parameters

Despite the long history of theoretical and computer modeling of the experimental results no unified set of microscopic parameters entering the Hamiltonian  $H$  has been revealed up to now [10–14, 16–20, 26].

The one-exciton band of the ideal ring  $E(k)$  consists of two groups of 9 transitions arranged asymmetrically relative to the zero local site energy. These Davydov manifolds appear because the 18 BChl molecules in the B850 ring are grouped into heterodimers with different coupling energies within the elementary dimers  $J_{12}$  and between them  $J_{23}$  as well as different local energies  $\epsilon_1 \neq \epsilon_2$ .

In the presence of static disorder ( $\Delta \neq 0$  in  $H_1$ ) virtually all exciton transitions gain strength at the expense of the low energy  $k = \pm 1$  transitions, which dominate the spectrum of the ideal B850 ring. There is still a discrepancy between the measurement by Freiberg et al. [11] and results of hole-burning experiments by Small (see references in [1]). In the former experiments considerable intensity of about 13% (averaged over a large ensemble) attained by the lowest  $k = 0$  transition has been revealed. In interpreting these experiments it was concluded [11] that the shape of the linear absorption spectrum of B850 at 8 K could be well reproduced by taking  $\Delta \approx 0.7$ . The hole burning results at 4 K imply much smaller disorder leading to a relative intensity of the  $k = 0$  subband of only 3%. The model parameters obtained by Freiberg from fitting the simulated linear and nonlinear absorption spectra to the low temperature experimental data are the transfer integrals  $J_{12} = 375 \text{ cm}^{-1}$  and  $J_{13} = 20 - 30 \text{ cm}^{-1}$  as well as the strength of the static disorder  $\Delta = 216 \text{ cm}^{-1}$  with FWHM =  $507 \text{ cm}^{-1}$ . The dynamic disorder leads to a broadening of the exciton levels  $E(k)$  with a FWHM =  $58 \text{ cm}^{-1} = J/6.5$ .

Novoderezhkin et al. [19, 20] fitted the pump-probe spectra of the LH2 antenna. Taking into account the difference between the local BChl energies  $\Delta\epsilon = \epsilon_1 - \epsilon_2$  in the basic dimer which leads to the splitting of the exciton energy band to two subbands, the following set of microscopic parameters : the transfer integrals  $J_{12} = 400 \text{ cm}^{-1}$ ,  $J_{23} = 290 \text{ cm}^{-1}$ , the homogeneous line widths of exciton states in the lower subband  $\Gamma_{1L} = 240 \text{ cm}^{-1}$  and in the higher subband  $\Gamma_{1H} = 340 \text{ cm}^{-1}$  and the strength of the static disorder  $\Delta = 450 \text{ cm}^{-1}$  has been used. Koolhaas et al. [14] have recently obtained the transfer integrals  $J_{12} = 396 \text{ cm}^{-1}$  and  $J_{23} = 300 \text{ cm}^{-1}$ .

In what follows we will use the transfer integral  $J_{12}$  as energy unit. We choose  $J_{23} = 0.7$ ,  $\Delta\epsilon = \epsilon_1 - \epsilon_2 = J_{12}$ , and  $\Delta$  between 0.2 and 1. To convert the time  $\tau$  in these units into seconds one has to divide  $\tau$  by  $2\pi c J_{12}$  with  $c$  the speed of light in cm/s and  $J_{12}$  in units of  $\text{cm}^{-1}$ . So  $\tau = 1$  corresponds to 21.2 fs for  $J_{12} = 250 \text{ cm}^{-1}$  and to 13.3 fs for  $J_{12} = 400 \text{ cm}^{-1}$ .

## 2.4 Nature of the initially prepared state

For a coplanar arrangement of site transition moments  $\vec{\mu}_n$  dipole-allowed transitions from the ground state populate only the degenerate  $k = \pm 1$  levels of the ideal (without dynamic and static disorders) ring with Hamiltonian  $H_{ex}^0$  and eigenstates  $|k\rangle$ . If static disorder of the local energies is present ( $\Delta \neq 0$ ), the stationary states, i.e. the eigenstates  $|a\rangle$  of the Hamiltonian  $H_{ex}^0 + H_1$ , correspond to mixtures of  $|k\rangle$  and an excitation will prepare a superposition



of the  $|k\rangle$  states.

However, Kumble and Hochstrasser [24] concluded, that in the case of pump-pulse excitation the dipole strength is simply redistributed among the exciton levels due to disorder. So the amplitudes of site excitations and the phase relationships in the initial state are necessarily identical to that of an equal superposition of  $k = \pm 1$  excitons of the ideal ring. Thus, generally, the excitation with a pump pulse of sufficiently wide spectral bandwidth will always prepare the same initial state, irrespective of the actual eigenstates of the system. The nature of this initial state is entirely determined by the selection rules of the unperturbed system.

We shall use the following definitions for the dipole strength

$$\vec{\mu}_a = \sum_{n=1}^N c_n^a \vec{\mu}_n \quad (7)$$

of state  $|a\rangle$  of the real system and for the dipole strength

$$\vec{\mu}_\alpha = \sum_{n=1}^N c_n^\alpha \vec{\mu}_n \quad (8)$$

of state  $|\alpha\rangle$  of the ideal crystal. The coefficients  $c_n^\alpha$  and  $c_n^l$  are the expansion coefficients of the eigenstates of the ideal and disordered aggregates in site representation.

The pump pulse is characterized by the polarization unit vector  $\vec{e}_i$ . Then the initial condition for the density matrix by pulse excitation with the polarization  $\vec{e}_i$  is given by (Eq. (1a) in [15]):

$$\rho_{\alpha\beta}(t=0; \vec{e}_i) = \frac{1}{A} (\vec{e}_i \cdot \vec{\mu}_\alpha) (\vec{e}_i \cdot \vec{\mu}_\beta), \quad (9)$$

where  $A = \sum_\alpha (\vec{e}_i \cdot \vec{\mu}_\alpha) (\vec{e}_i \cdot \vec{\mu}_\alpha)$ . This initial condition for pulse excitation [24] should be expressed in the eigenstate basis of the real system:

$$\begin{aligned} \rho_{ab}(t=0; \vec{e}_i) &= \sum_\alpha \sum_\beta \langle a|\alpha\rangle \rho_{\alpha\beta}(t=0; \vec{e}_i) \langle \beta|b\rangle \\ &= \frac{1}{A} \sum_\alpha \sum_\beta (\vec{e}_i \cdot \vec{\mu}_\alpha) (\vec{e}_i \cdot \vec{\mu}_\beta) \langle a|\alpha\rangle \langle \beta|b\rangle, \end{aligned} \quad (10)$$

From (10) one obtains

$$\begin{aligned} \rho_{ab}(t; \vec{e}_i) &= e^{-\frac{i}{\hbar}t(E_a-E_b)} \rho_{ab}(t=0; \vec{e}_i) \\ &= \frac{1}{A} e^{-\frac{i}{\hbar}t(E_a-E_b)} \sum_\alpha \sum_\beta (\vec{e}_i \cdot \vec{\mu}_\alpha) (\vec{e}_i \cdot \vec{\mu}_\beta) \langle a|\alpha\rangle \langle \beta|b\rangle. \end{aligned} \quad (11)$$

## 2.5 Static disorder-induced scattering of the initially pure state

Pump-probe and spontaneous emission measurements on the femtosecond time scale have revealed ultrafast depolarization in the core and peripheral ASs with biphasic kinetics: a fast sub-100 fs component and a slower decay on a 200–400 fs time scale were observed in all cases [1]. Kumble and Hochstrasser [24] thoroughly investigated the time dependence of the disorder-induced scattering of the initial state  $|k \pm 1\rangle$ . The evolution of the initially delocalized exciton

$$P_k(t) = |\langle k | e^{-\frac{i}{\hbar} H t} | k \rangle|^2 \quad (12)$$

has been followed considering only the influence of a static uncorrelated distribution of the local site energies in a circular aggregate.

In the basis  $|k\rangle$  of the ideal ring the time evolution can be described as scattering of the initially prepared exciton  $|k = \pm 1\rangle$  into those levels to which it is coupled by the presence of disorder. The nonexponential nature of scattering dynamics has been demonstrated: for  $\Delta = J/3.5$  the initial state decays in two distinct phases; a dominant  $\approx 100$  fs component and a slower (200–300 fs) decay are evident.

## 2.6 Consequences of the static disorder-induced scattering in optical anisotropy measurements

Optical anisotropy measurements provide a convenient mean to follow experimentally the decay of a virtual exciton within the LH2 ring. Since this initial state is prepared as a superposition of eigenstates of the aggregate, polarized pump-probe (or fluorescence) signals contain contributions from interference terms which last so long that the phase coherence between different levels is maintained. The decay of these cross terms directly reflects the time scale of electronic dephasing. In the present case it therefore represents the survival time of a virtual exciton within the disordered system.

Kumble and Hochstrasser [24] calculated the usual time-dependent anisotropy using

$$r(t) = \frac{\langle S_{xx}(t) \rangle - \langle S_{xy}(t) \rangle}{\langle S_{xx}(t) \rangle + 2\langle S_{xy}(t) \rangle} \quad (13)$$

where the brackets  $\langle \rangle$  denote the ensemble average and the average over the direction of the laser pulses with fixed relative directions  $\vec{e}_1$  and  $\vec{e}_2$ . For excitation and probe pulses which are polarized along the  $\vec{e}_x$  and  $\vec{e}_y$  directions, respectively, the transient gain signal from the delocalized initial state is given by [24]

$$\langle S_{xy}(t) \rangle = \langle \left| \sum_{\alpha, l, n} (\vec{e}_x \cdot \vec{\mu}_\alpha) (\vec{e}_y \cdot \vec{\mu}_l) c_n^{\alpha*} c_n^l e^{-i\omega_l t} \right|^2 \rangle \quad (14)$$

where the indices  $\alpha$  and  $l$  label the eigenstates of the virtual and disordered aggregates, respectively. The index  $n$  represents the individual site excitations. The gain signal  $\langle S_{xx}(t) \rangle$  is defined accordingly.

In Kumble and Hochstrasser's modeling, the decay of the initial state has been directly manifested itself as a depolarization reducing the anisotropy from 0.7 to 0.3 – 0.35 and a subsequent recurrence to establish a final value of 0.4. Kumble and Hochstrasser supposed that equilibration between eigenstates of the aggregate would lead to a further decrease of the anisotropy to  $\approx 0.1$ , but this process has not been considered in their paper [24]. They estimated, by comparison of their results with experiment, that the static disorder in a LH2 ring has a value of  $\Delta \approx 0.4 - 0.8$  which should be considered as an upper limit since dynamic variations of the relative eigenstate energies occurring on a 100 fs time scale would contribute to the scattering process.

## 2.7 Effects of the dynamical disorder

As pointed out in Sec. 1 the aim of the present paper is to extend the above described theory given in Ref. [24] by including the effect of dynamic scattering which contributes to dephasing of the initial wave packet and promotes a thermalization of the dephased populations. To deal with the dynamic disorder, one works within the exciton density matrix formalism instead of using only the exciton wave functions.

Taken only those terms into account which are directly connected to the polarization the time-resolved fluorescence  $P_{if}(\omega, t)$  with initial  $\vec{e}_i$  and final polarization  $\vec{e}_f$  of the light is given (cf. Chapter 3, Eq. (2.58) in [27]) in our notation as

$$P_{if}(\omega, t) = A \sum_l \sum_{l'} \rho_{ll'}(t) (\vec{e}_f \cdot \vec{\mu}_{l'}) (\vec{e}_f \cdot \vec{\mu}_l) [\delta(\omega - \omega_{l'0}) + \delta(\omega - \omega_{l0})] =$$

$$A \sum_l \sum_{l'} \rho_{ll'}(t) \sum_k \sum_j (\vec{e}_f \cdot \vec{\mu}_k) (\vec{e}_f \cdot \vec{\mu}_j) \langle j|l \rangle \langle l'|k \rangle [\delta(\omega - \omega_{l'0}) + \delta(\omega - \omega_{l0})] \quad (15)$$

and in case of no interaction with a bath as

$$P_{if}(\omega, t) =$$

$$\sum_l \sum_{l'} \sum_\alpha \sum_\beta e^{-\frac{i}{\hbar} t (E_l - E_{l'})} (\vec{e}_i \cdot \vec{\mu}_\alpha) (\vec{e}_i \cdot \vec{\mu}_\beta) \langle l|\alpha \rangle \langle \beta|l' \rangle (\vec{e}_f \cdot \vec{\mu}_{l'}) (\vec{e}_f \cdot \vec{\mu}_l) \times$$

$$[\delta(\omega - \omega_{l'0}) + \delta(\omega - \omega_{l0})]. \quad (16)$$

This expression can be directly rewritten (after integration over  $\omega$ ) in the form of Kumble and Hochstrasser:

$$S_{ij}(t) = \int P_{if}(\omega, t) d\omega =$$

$$\int \sum_l \sum_{l'} \sum_\alpha \sum_\beta e^{-\frac{i}{\hbar} t (E_l - E_{l'})} (\vec{e}_i \cdot \vec{\mu}_\alpha) (\vec{e}_i \cdot \vec{\mu}_\beta) \langle l|\alpha \rangle \langle \beta|l' \rangle (\vec{e}_f \cdot \vec{\mu}_{l'}) (\vec{e}_f \cdot \vec{\mu}_l)$$

$$\times [\delta(\omega - \omega_{l'0}) + \delta(\omega - \omega_{l0})] d\omega =$$

$$\int \sum_l \sum_{l'} \sum_\alpha \sum_\beta e^{-\frac{i}{\hbar} t (E_l - E_{l'})} \times$$

$$\begin{aligned}
& (\vec{e}_i \cdot \vec{\mu}_\alpha)(\vec{e}_i \cdot \vec{\mu}_\beta) \sum_n \sum_{n'} \langle l|n \rangle \langle n|\alpha \rangle \langle \beta|n' \rangle \langle n'|l' \rangle (\vec{e}_f \cdot \vec{\mu}_{l'}) (\vec{e}_f \cdot \vec{\mu}_l) [\delta(\omega - \omega_{l'0}) + \delta(\omega - \omega_{l0})] d\omega = \\
& \left( \sum_\alpha \sum_l \sum_n (\vec{e}_i \cdot \vec{\mu}_\alpha)(\vec{e}_f \cdot \vec{\mu}_l) \langle l|n \rangle \langle n|\alpha \rangle e^{-i\omega_l t} \right) \times \\
& \left( \sum_\beta \sum_{l'} \sum_{n'} (\vec{e}_i \cdot \vec{\mu}_\beta)(\vec{e}_f \cdot \vec{\mu}_{l'}) \langle \beta|n' \rangle \langle n'|l' \rangle e^{i\omega_{l'} t} \right) = \\
& \left| \sum_{\alpha, l, n} (\vec{e}_i \cdot \vec{\mu}_\alpha)(\vec{e}_f \cdot \vec{\mu}_l) \langle \alpha|n \rangle \langle n|l \rangle e^{-i\omega_l t} \right|^2. \tag{17}
\end{aligned}$$

We see, that the crucial quantity entering the time dependence of the anisotropy is the exciton density matrix. In the next section we shall therefore review several methods leading to dynamic equations for the exciton density matrix which include microscopically the interaction of the exciton with the bath. They could be obtained from, e.g., the general Tokuyama-Mori approach only by serious approximations. One of them is the Redfield model with and without the so-called secular approximation [28,29], which has been applied to exciton transfer and relaxation problems in AS rings several times. It has been shown [30,31] that in contrast to the justification of the secular approximation, the non-secular terms do not average out in time.

Our result, presented in section 4, have therefore been obtained with the Redfield model without secular approximation.

### 3 Dynamic equations for the reduced exciton density matrix

The bath-related relaxation can be described in a variety of ways. Among others these are the path integral methods [32,33], the semigroup methods [34–36], and the reduced density matrix (RDM) theory [37]. Here we concentrate on the latter.

Having defined the Hamiltonian  $H$  of the system, one exciton and a bath, one has to solve the equations of motion for the complete density matrix  $\sigma$ , namely the Liouville equation

$$i\hbar \frac{\partial}{\partial t} \sigma(t) = L\sigma. \tag{18}$$

This is not a simple task because one has to find the time development of all matrix elements of the density matrix - diagonal and off-diagonal - in any representation which takes into account the exciton and phonon states.

Nevertheless, this treatment is not necessary in many cases. Information, which is used in further investigations, is in many cases limited. For example, the site occupation probabilities  $P_m(t)$  of the exciton (the diagonal matrix elements in site representation after averaging over the bath variables) are in many cases the most interesting quantities in theoretical investigations of the

exciton transfer. The transfer problem of, e.g. a Frenkel exciton interacting with a bath, is usually treated by projecting out the bath degrees of freedom. This yields dynamic equations for the single-exciton density matrix  $\rho$  complementing the usual single-exciton Liouville equation by terms describing the bath influence. The latter terms must, on the other hand, be properly parametrized.

### 3.1 Stochastic theories

In the stochastic treatment of the exciton interaction with the dynamic and static disorders the influence of disorder is described by a stochastic process, i.e. the interaction part of the microscopic Hamiltonian is replaced by a stochastic time-dependent model Hamiltonian. In the original version [38] of the stochastic Liouville equation method (SLE) the bare exciton is influenced by a stochastic field

$$H_2(t) = \sum_{m,n} h_{mn}(t) a_m^+ a_n. \quad (19)$$

Grover and Silbey [39] suggested that one could understand the excitation in molecular aggregates also as a fully dressed exciton (polaron) obtained from the microscopic Hamiltonian using a canonical transformation. The stochastic field acting on the dressed excitation has a different microscopic meaning as that one acting on the bare exciton [40]. The stochastic field obtained from the microscopic Hamiltonian for the local and linear exciton-phonon interaction leads [40], in the bare exciton representation, mainly to local energy fluctuations while the corresponding stochastic field acting on the polaron leads mainly to fluctuations of the renormalized transfer integrals.

The exciton-phonon interaction in the ring subunits LH1 and LH2 of the purple bacteria should not be very strong [1]. Then the Hamiltonian  $H_2(t)$  models the influence of dynamic disorder mainly via fluctuations of the local exciton energies  $h_{mm}(t)$ . Mean values and correlation functions are given by

$$\begin{aligned} \langle h_{mm}(t) \rangle &= 0, \\ \langle h_{nn}(t) h_{mm}(\tau) \rangle &= \delta_{mn} \Delta^2 \exp(-\lambda |t - \tau|). \end{aligned} \quad (20)$$

Multitime correlation functions entering the equations of motion can be calculated from two-time correlation functions (20) according to different rules. Mostly dichotomic, Gaussian and white noise statistics have been applied in the past.

The simplest description of the exciton dynamics in the framework of the stochastic theories is obtained in the so-called white noise limit  $\Delta^2/\lambda \rightarrow \gamma_0$  ( $\Delta \rightarrow \infty$ ,  $\lambda \rightarrow \infty$ ) in which the time correlation functions become  $\delta$  functions. The SLE for the bare exciton density matrix in the Haken-Strobl-Reineker parametrization (HSR-SLE) (for a review, see [38]) have been used very often to describe the coupled coherent and incoherent regime of exciton transfer in

molecular aggregates using a few phenomenological parameters  $\gamma$ :

$$\begin{aligned}
\frac{\partial}{\partial t}\rho_{mn}(t) &= -\frac{i}{\hbar}([H_0, \rho(t)])_{mn} \\
&\quad + 2\delta_{mn} \sum_p [\gamma_{mp}\rho_{pp}(t) - \gamma_{pm}\rho_{mm}(t)] \\
&\quad - (1 - \delta_{mn})[2\Gamma_{mn}\rho_{mn}(t) - 2\bar{\gamma}_{mn}\rho_{nm}], \\
2\Gamma_{mn} &= \sum_p (\gamma_{pm} + \gamma_{pn}) = 2\Gamma_{nm}.
\end{aligned} \tag{21}$$

In most applications of the HSR-SLE nearest neighbor parameters  $\gamma_0 = \gamma_{nm}$  for  $n = m$ ,  $\gamma_1 = \gamma_{nm}$  for  $n = m \pm 1$  and  $\bar{\gamma}_1 = \bar{\gamma}_{nm}$  for  $n = m \pm 1$  have been used. We have shown [40] that in case of a weak interaction which is site-diagonal and linear in the lattice displacements only  $\gamma_0 \neq 0$ . Such treatment has been used by us [42–44] and Leegwater [41] in the investigation of exciton transfer in ring structures.

## 3.2 Redfield theory

Provided that the excitation dynamics is not very fast, the coupling is rather weak, the bath and the system are initially statistically independent, and except for the initial time-interval  $t \lesssim t_d$  ( $t_d$  = dephasing time of the bath), the approximate equation turns to the form first derived by Redfield [28, 29]:

$$i\frac{d}{dt}\rho(t) = \frac{1}{\hbar}[H, \rho(t)] + \mathcal{R}\rho(t), \tag{22}$$

where the Redfield relaxation superoperator  $\mathcal{R}$  (as a linear time-independent superoperator) describes the influence of dynamics of the medium and its interaction with the exciton. In the modern fashion, derivation of Eq. (22) is perhaps best presented in [37] or [45]. In the basis of eigenstates  $|\mu\rangle, |\nu\rangle, \dots$  of the relevant system part the Redfield theory reads

$$\frac{d}{dt}\rho_{\mu\nu}(t) = -\frac{i}{\hbar}E_{\mu\nu}\rho_{\mu\nu}(t) + \sum_{\mu'\nu'} \mathcal{R}_{\mu\nu\mu'\nu'}\rho_{\mu'\nu'}(t) \tag{23}$$

where  $E_{\mu\nu} = E_\mu - E_\nu = \hbar\omega_{\mu\nu}$ . The physical interpretation of the so-called Redfield tensor  $\mathcal{R}_{\mu\nu\mu'\nu'}$ , is straightforward: Each element is essentially a rate constant that relates the rate of change of reduced density matrix elements  $\rho_{\mu\nu}$  to the current value of the other matrix element  $\rho_{\mu'\nu'}$ . Thus  $\mathcal{R}_{\mu\mu\mu\mu}$  is the relaxation rate of the depopulation of eigenstate  $|\mu\rangle$  while  $\mathcal{R}_{\mu\mu\nu\nu}$  represents the rate of population transfer from state  $|\nu\rangle$  to the state  $|\mu\rangle$ . The elements  $\mathcal{R}_{\mu\nu\mu\nu}$  represent the dephasing rates of the off-diagonal density matrix elements  $\rho_{\mu\nu}$ . An important property of the Redfield tensor is that when the bath is treated quantum mechanically, the physically required detailed balance conditions are naturally satisfied, so that the subsystem relaxes to thermal equilibrium with

the bath. This condition means that the ratio of forward and reverse rate constants between states  $|\mu\rangle$  and  $|\nu\rangle$  is

$$\frac{\mathcal{R}_{\mu\mu\nu\nu}}{\mathcal{R}_{\nu\nu\mu\mu}} = \exp(-\beta\hbar\omega_{\mu\nu}) . \quad (24)$$

Other elements of the Redfield tensor cannot be given such a simple interpretation. Keeping them as just fitting semi-empirical parameters leads to technical complications as the total number of elements of  $\mathcal{R}$  increases as  $N^4$  ( $N$  is the number of eigenstates involved, i.e. two for the dimer). Hence, the idea is to omit those elements of  $\mathcal{R}$  which are physically less relevant provided that this omission does not appreciably influence the solution. That is why already Redfield himself [28, 29] suggested the so-called secular approximation. This approximation amounts to neglecting those elements of  $\mathcal{R}$  that couple elements of the density matrix  $\rho_{\mu'\nu'}$  with incommensurate frequencies  $E_{\mu\nu}/\hbar$  determined in the first term on the right hand side of (23). In other words, it means to put  $R_{\mu\nu\mu'\nu'} = 0$  whenever  $E_{\mu\nu} \neq E_{\mu'\nu'}$ . It has been shown [30, 31] that this approximation leads to non-physical effects in the transfer processes and is thus, in spite of its apparent success in many cases, physically not acceptable if we discuss, e.g., relaxation among states other than eigenstates of the Hamiltonian of the system. Other approximations to the Redfield theory, which have not been applied here, have been used and tested in the context of electron transfer [31, 46]. Aspects concerning the efficient numerical implementation of the Redfield equation are discussed elsewhere [47].

Although being aware that Redfield theory is limited to the high temperature regime i.e. the system relaxation times have to be large compared to the thermal time  $\hbar/(k_b T)$  we assume here that this theory gives reasonable results also at low temperatures. In the present study Redfield theory is applied to the full temperature range.

### 3.3 Generalizations of the HSR-SLE method in the local representation

The original HSR-SLE method [38] represents the simplest stochastic treatment of the microscopic interaction Hamiltonian, but the application of the white noise is very restrictive. It leads to improper long time asymptotics of the occupation probabilities of the extended exciton states  $P_k(\infty)$ . Many attempts have been made to determine more general equations using different representations of the exciton interacting with the bath and different ways of obtaining the dynamic equations for the exciton density matrix from the full Hamiltonian (1). The equations obtained in such a way could, after some further approximations and manipulations, be rewritten [48–50] in a form which resembles the nonconvolutional SLE but brings several important improvements.

Čápek [48–50] applied several different ways of obtaining of the convolutional and convolutionless dynamical equations for the exciton density matrix.

The equations of motion obtained read

$$\frac{d}{dt}\rho_{mn}(t) = \sum_{pq} i\omega_{mn,pq}(t)\rho_{pq}(t), \quad (25)$$

where

$$\omega_{mn,pq}(t) = \Omega_{mn,pq} + \delta\Omega_{mn,pq}(t). \quad (26)$$

When the typical system times are much longer than the bath correlation time, i.e. in the Markovian limit, one obtain a system of equations with constant coefficients

$$\begin{aligned} \Omega_{mn,pq} &= \frac{1}{\hbar}[\delta_{mp}\delta_{nq}(\epsilon_n - \epsilon_m) + J_{qn}\delta_{mp} - J_{mp}\delta_{nq}], \\ i\delta\Omega_{mn,pq} &= -\delta_{mp}\mathcal{A}_{nm}^q - \delta_{nq}\mathcal{A}_{mn}^{p*}, \\ \mathcal{A}_{mn}^p &= \frac{i\hbar}{N} \sum_k \omega_k^2 (G_{-k}^m - G_{-k}^n) \sum_r G_k^r \sum_{\nu_1, \nu_2} \langle \nu_2 | r \rangle \langle r | \nu_1 \rangle \langle \nu_1 | m \rangle \langle p | \nu_2 \rangle \times \\ &\quad \left\{ \frac{1 + n_B(\hbar\omega_k)}{E_{\nu_1} - E_{\nu_2} + \hbar\omega_k + i\varepsilon} + \frac{n_B(\hbar\omega_k)}{E_{\nu_1} - E_{\nu_2} - \hbar\omega_k + i\varepsilon} \right\}. \end{aligned} \quad (27)$$

Here  $|\nu\rangle$  and  $E_\nu$  label the corresponding eigenvalues and eigenvectors of  $H_{ex}^0$ . Čápek suggested the parametrization

$$A_{mn}^p = \text{Re } \mathcal{A}_{mn}^p, \quad B_{mn}^p = \text{Im } \mathcal{A}_{mn}^p. \quad (28)$$

In the fast carrier regime the coefficients  $B_{mn}^p$  become negligible (no renormalization of  $J_{mn}$ ) and can be omitted.

The  $A_{mn}^m$  play the same role as the coefficient  $\gamma_0 \equiv \gamma_{mm}$  of the HSR parametrization. The coefficients  $A_{mn}^n$  provide the bath-induced coupling of to the off-diagonal to diagonal elements of  $\rho_{mn}(t)$ .

## 4 Results

### 4.1 Equivalence of Redfield and Čápek's equations

We have used the dynamical equations of motion for the reduced exciton density matrix in the Čápek's form (25) and (26) to express the time dependence of the optical properties of the model LH2 ring of BChls in the fs time range.

For linear local exciton-phonon coupling the Hamiltonian  $H_{ex-ph}$  can be written as

$$H_{ex-ph} = \sum_m K_m \Phi_m, \quad (29)$$

where the system operators  $K_m$  and bath operators  $\Phi_m$  are given by

$$K_m = a_m^\dagger a_m, \quad \Phi_m = \frac{\hbar}{\sqrt{N}} \sum_q G_q^m \omega_q (b_q^\dagger + b_q).$$



If we express the equation of motion for the reduced density matrix in Born approximation (second order in exciton-bath coupling) in terms of  $K_m$  and  $\Phi_m$ , and apply the Markov approximation (in the interaction picture), the dissipation term looks like [45]

$$\left(\frac{\partial \rho}{\partial t}\right)_{diss} = -\frac{1}{\hbar^2} \sum_{m,n} \int_0^\infty d\tau \left\{ C_{mn}(\tau) \left[ K_m, K_n^{(I)}(-\tau) \rho(t) \right]_- \right. \\ \left. - C_{mn}^*(\tau) \left[ K_m, \rho(t) K_n^{(I)}(-\tau) \right]_- \right\}, \quad (30)$$

where  $C_{mn}(t)$  is the bath correlation function

$$C_{mn}(t) = \langle \Phi_m(t) \Phi_n(0) \rangle_B. \quad (31)$$

Here we assume that the expectation values  $\langle \Phi_m \rangle$  vanish. The original Redfield equations are derived in eigenstate representation [28, 29]. Here we will express Eq. (30) in site representation

$$\left(\frac{\partial \rho_{rs}}{\partial t}\right)_{diss} = -\frac{1}{\hbar^2} \sum_{m,n} \int_0^\infty d\tau \left\{ C_{mn}(\tau) \sum_{i,j} \left( \langle r | K_m | i \rangle \langle i | K_n^{(I)}(-\tau) | j \rangle \rho_{js}(t) - \right. \right. \\ \left. \langle r | K_n^{(I)}(-\tau) | i \rangle \langle j | K_m | s \rangle \rho_{ij}(t) \right) \\ \left. - C_{mn}^*(\tau) \sum_{i,j} \left( \langle r | K_m | i \rangle \langle j | K_n^{(I)}(-\tau) | s \rangle \rho_{ij}(t) - \right. \right. \\ \left. \left. \langle i | K_n^{(I)}(-\tau) | j \rangle \langle j | K_m | s \rangle \rho_{ri}(t) \right) \right\}, \quad (32)$$

where the indices  $i, j, r, s$  denote sites.

For  $K_m$  as given above we have

$$\langle r | K_m | s \rangle = \delta_{rm} \delta_{sm}. \quad (33)$$

Using the simple expression for the time evolution operator  $U(\tau)$  in energy representation  $\langle \alpha | U(\tau) | \beta \rangle = \delta_{\alpha\beta} e^{-\frac{i}{\hbar} \varepsilon_\alpha \tau}$  one gets

$$\langle r | K_m^{(I)}(-\tau) | s \rangle = \langle r | U(\tau) K_m U^\dagger(\tau) | s \rangle = \\ \sum_{i,j} \sum_{\alpha,\beta} \langle r | \alpha \rangle e^{-\frac{i}{\hbar} \varepsilon_\alpha \tau} \langle \alpha | i \rangle \delta_{in} \delta_{jn} \langle j | \beta \rangle e^{\frac{i}{\hbar} \varepsilon_\beta \tau} \langle \beta | s \rangle = \sum_{\alpha,\beta} \langle r | \alpha \rangle \langle \alpha | n \rangle \langle n | \beta \rangle \langle \beta | s \rangle e^{-i\omega_{\alpha\beta}\tau}. \quad (34)$$

In this treatment the matrix elements of  $K_m^{(I)}$  are evaluated exactly. In the context of electron transfer the so-called *adiabatic damping approximation* has been used and tested [31, 46]. In this approximation the influence of the site coupling on dissipation is neglected.

After substituting Eqs. (33) and (34) into (32) the final form of the equation of motion for the reduced density matrix in local site representation reads

$$\begin{aligned} \left( \frac{\partial \rho_{rs}}{\partial t} \right)_{diss} &= -\frac{1}{\hbar^2} \sum_{n,j} \sum_{\alpha,\beta} \int_0^\infty d\tau e^{-i\omega_{\alpha\beta}\tau} \\ &\times \{ (C_{rn}(\tau) - C_{sn}(\tau)) \langle r|\alpha \rangle \langle \alpha|n \rangle \langle n|\beta \rangle \langle \beta|j \rangle \rho_{js}(t) \\ &- (C_{rn}^*(\tau) - C_{sn}^*(\tau)) \langle j|\alpha \rangle \langle \alpha|n \rangle \langle n|\beta \rangle \langle \beta|s \rangle \rho_{rj}(t) \}. \end{aligned} \quad (35)$$

If one now introduces the parameters  $\mathcal{A}_{rs}^m$

$$\mathcal{A}_{rs}^m = \frac{1}{\hbar^2} \sum_{\alpha,\beta} \int_0^\infty d\tau e^{-i\omega_{\alpha\beta}\tau} \sum_n (C_{sn}^*(\tau) - C_{rn}^*(\tau)) \langle m|\alpha \rangle \langle \alpha|n \rangle \langle n|\beta \rangle \langle \beta|r \rangle \quad (36)$$

it is possible to express Eq. (35) in the same form as it was done by Čápek [50]:

$$\left( \frac{\partial \rho_{rs}}{\partial t} \right)_{diss} = i\delta\Omega_{rs,pq} \rho_{pq}, \quad (37)$$

where

$$i\delta\Omega_{rs,pq} = -\delta_{rp} \mathcal{A}_{sr}^q - \delta_{sq} \mathcal{A}_{rs}^{p*}. \quad (38)$$

So Redfield theory without secular approximation and Čápek's theory after Markov approximation are equivalent.

In what follows we have used a simple model for  $C_{mn}$ . Each site (chromophore) has its own bath with one bath coordinate, and the various coordinates are completely uncorrelated. Further it is assumed that these baths have identical properties [1, 45]. Then only one correlation function  $C(\omega)$  is needed

$$C_{mn}(\omega) = \delta_{mn} C(\omega), \quad (39)$$

with

$$C_{mn}(\omega) = \int_{-\infty}^\infty C_{mn}(\tau) e^{i\omega\tau} d\tau = 2\text{Re} \int_0^\infty C_{mn}(\tau) e^{i\omega\tau} d\tau. \quad (40)$$

In case of real eigenvectors (which always can be chosen for this system)  $\langle m|\alpha \rangle$  and if we omit the imaginary parts of  $\mathcal{A}_{rs}^m$  which cause only renormalization of transfer integrals  $J$  [50], we can write

$$A_{rs}^m = \text{Re} \mathcal{A}_{rs}^m = \frac{1}{2\hbar^2} \sum_{\alpha\beta} C(\omega_{\alpha\beta}) \langle m|\alpha \rangle \langle \beta|r \rangle (\langle \alpha|s \rangle \langle s|\beta \rangle - \langle \alpha|r \rangle \langle r|\beta \rangle) \quad (41)$$

and after introduction of the spectral density  $J(\omega)$  [45]

$$C(\omega) = 2\pi\hbar^2 [1 + n_B(\omega)] [J(\omega) - J(-\omega)], \quad (42)$$

it is possible to write

$$\begin{aligned} A_{rs}^m &= -\pi \sum_{\alpha\beta} [1 + n_B(\omega_{\alpha\beta})] [J(\omega_{\alpha\beta}) - J(\omega_{\beta\alpha})] \times \\ &\quad \langle m|\alpha \rangle \langle \beta|r \rangle (\langle \alpha|s \rangle \langle s|\beta \rangle - \langle \alpha|r \rangle \langle r|\beta \rangle) \\ &= -\pi \sum_{\alpha\beta(\varepsilon_\beta > \varepsilon_\alpha)} J(\omega_{\alpha\beta}) (\langle \alpha|s \rangle \langle s|\beta \rangle - \langle \alpha|r \rangle \langle r|\beta \rangle) \times \\ &\quad \{ [1 + n_B(\omega_{\alpha\beta})] \langle m|\alpha \rangle \langle \beta|r \rangle + n_B(\omega_{\alpha\beta}) \langle m|\beta \rangle \langle \alpha|r \rangle \}. \end{aligned} \quad (43)$$

In the following we have modeled the spectral density by the form usually used dealing with the BCHs in the LH2 ring unit [1, 25, 45]

$$J(\omega) = \Theta(\omega) j_0 \frac{\omega^2}{2\omega_c^3} e^{-\omega/\omega_c}. \quad (44)$$

It has its maximum at  $2\omega_c$ . We shall use (in agreement with [25])  $j_0 = 0.2$  or  $j_0 = 0.4$  and  $\omega_c = 0.2$ .

## 4.2 Disorder-induced scattering of the initial state

In the unperturbed ring the time evolution of a exciton in the presence of static site energy and dynamic disorder leads to a loss of its coherent characteristics, i.e., destruction of the phase relationships between the individual eigenstates comprising the initial wave packet state. We have calculated the time dependence of the occupation probability of the initial state after impulsive excitation, namely

$$P_k(t) = \rho_{kk}(t) \quad (45)$$

for an equal superposition of  $k = \pm 1$  states. In the basis of the unperturbed system the time evolution can be described as scattering of the initially prepared exciton into the levels to which it is coupled by the presence of disorder. The scattering dynamics of a single ring after averaging over more than 1000 realizations of the static disorder  $\Delta$  is shown in Fig. 1 for four static disorders. The influence of the dynamic disorder is displayed for different temperatures for three values of dissipation. The curves (i) with no dissipation do not coincide with the corresponding results by Kumble and Hochstrasser, Fig. 2 in [24]. Their figures correspond to the time dependence of  $P_{+1}(t)$  or  $P_{-1}(t)$ . In Fig. 1 one can see a pronounced effect of the dynamic disorder (curves (ii) - (v)) on the disorder-induced scattering of the initial state, while the results without dynamic disorder (the Redfield tensor set to zero) (i) coincide with those of Kumble and Hochstrasser [24] (when comparing the time dependence of  $P_{+1}(t)$  or  $P_{-1}(t)$  with Fig. 2 in Ref. [24]). With dissipation the populations equilibrate while without dissipation the populations first decay rapidly but then increase again. Without static and dynamic disorder this would lead to full revivals. For short times some reminiscences of these revivals are seen if one neglects dissipation. For low temperatures (cases (ii), (iv)), the dynamic disorder leads to a further decay of the occupation probabilities  $P_{1,-1}(t)$  after an initial fast decay. Low temperature correspond to  $k_B T / J_{12} = 0.001$  i.e. for  $J_{12} = 250 \text{ cm}^{-1}$  the temperature is  $T = 0.36 K$ . For room temperature the inclusion of dynamic disorder leads to faster initial decay.

## 4.3 Consequences of the disorder-induced scattering in optical anisotropy measurements

The time-dependent anisotropy (13) has been calculated for excitation pulses polarized along the  $e_x$  directions ( $\vec{e}_i = \vec{e}_x$ ) and probe pulses which are polarized

along the  $e_x$  and  $e_y$  directions ( $\vec{e}_f = \vec{e}_x$  and  $\vec{e}_f = \vec{e}_y$ ). It is shown in Fig. 2. Similar conclusions as for Fig. 1 can be drawn from Fig. 2. It was concluded in Ref. [24] based on measurements by Chachisvilis et al. [51] that the time decay of the anisotropy during the first dozens of fs is *temperature independent* in the case of LH2 subunits. Our calculation show that such result can be obtained only for  $\Delta > 0.8$ . But because the time resolution of the experiments in [51] was not too high this very restrictive statement about the strength of the static disorder can only be made with caution. We expect that some temperature dependence can be seen using experiments with shorter laser pulses.

## 5 Discussion and concluding remarks

We have used the LH2 ring structure of real antenna subunits of purple bacteria photosynthetic systems as a motivation for our investigation of the time dependent optical spectra of our molecular aggregate ring model. In a series of papers the steady state optical absorption line shape of the Frenkel excitons on cyclic model oligomers have been calculated [6, 7] in presence of both dynamic and quasistatic disorders. Correlation with Freiberg's experimental data gives an estimate for the strength of the static disorder  $\Delta = 0.7$  [52].

In the present investigation we study the time-dependent optical properties under the influence of two simultaneous site energy fluctuations - quasistatic and dynamic within the LH2 ring antenna subunits of purple bacteria PSUs. Despite a long history of experimental and theoretical investigations no final conclusion has been done on the ratio  $\Delta/J_{12}$ . Kumble and Hochstrasser concluded to reach a decay in time-dependent optical experiments below 100 fs one needs  $\Delta \approx 0.4 - 0.8 J_{12}$ . They did not include dynamic disorder in their calculations. We have extended those calculations by including dissipation. We were able to show that in this case smaller values of  $\Delta/J_{12}$  are necessary than predicted by Kumble and Hochstrasser.

Our investigation has been based on several simplifications:

A) The time development of the reduced exciton density matrix has been described by the long time limit of Čápek's dynamical equations of motion (Markovian limit). As shown in this paper Čápek's equations are equivalent to the Redfield equation without secular approximation. More precise description of the time development of the exciton density matrix during first dozens of fs requires certainly more advanced description with time dependent coefficients in Eq. (25) (non-Markovian treatment). We had discussed such results obtained by us only for a dimer using different methods for description of the time development of the exciton density matrix [53]. In addition we have assumed that Redfield theory could give reasonable results for low temperature.

B) We have used the ring symmetry to describe the polarization properties of the Frenkel exciton states. Recent results obtained by single molecule spectroscopy [54] can only be interpreted [55] admitting the presence of a  $C_2$  distortion of the ring. It has, up to now, not been concluded whether such

$C_2$  distortion of the LH2 ring is present also in samples in vivo. Calculations which take into account the possible  $C_2$  distortion of the ring are on the way.

C) Kumble and Hochstrasser have pointed out that the information needed for a complete description of the exciton bath interaction is not available for the LH2 units. We have worked with a form of the spectral density which has been commonly used previously [1,25,45]. Work on a better description of the exciton–phonon interaction model is in progress.

## Acknowledgements

This work has been partially funded by contracts GAČR202/98/0499 and GAUK345/1998 and by the BMBF and DFG. While preparing this work, I.B. and P.H. experienced the kind hospitality of the Chemnitz University of Technology and U.K. experienced the kind hospitality of the Charles University in Prague.

## References

- [1] V. Sündström, T. Pullerits and R. van Grondelle, J. Phys. Chem. B 103 (1999) 2327.
- [2] P. Heřman, I. Barvík, J. Phys. Chem. B 103 (1999) 10892.
- [3] T. Renger, V. May, O. Kühn, Phys. Rep. 343 (2001) 137.
- [4] G. McDermott, S.M. Prince, A.A. Freer, A.M. Hawthornthwaite-Lawless, M.Z. Papiz, R.J. Cogdell, N.W. Issacs, Nature 374 (1995) 517.
- [5] A.A. Freer, S.M. Prince, K. Sauer, M.Z. Papiz, A.M. Hawthornthwaite-Lawless, G. McDermott, R.J. Cogdell, N.W. Issacs, Structure 4 (1996) 564.
- [6] I. Barvík, Ch. Warns, P. Reineker, J. Luminiscence 76&77 (1998) 331.
- [7] I. Barvík, Ch. Warns, Th. Neidlinger, P. Reineker, Chem. Phys. 240 (1999) 173 and 255 (2000) 403.
- [8] L.D. Bakalis, M. Coca, and J. Knoester, J. Lum. 76 & 77 (1998) 359.
- [9] L.D. Bakalis, M. Coca, and J. Knoester, J. Chem. Phys. 110 (1999) 2208.
- [10] A. Freiberg, J.A. Jackson, S. Lin, N.W. Woodbury, J. Phys. Chem. A 102 (1998) 4372.
- [11] A. Freiberg, K. Timpmann, S. Lin, N.W. Woodbury, J. Phys. Chem. B 102 (1998) 10974.
- [12] A. Freiberg, K. Timpmann, R. Ruus, N.W. Woodbury, J. Phys. Chem. B 103 (1999) 10032.
- [13] K. Timpmann, N.W. Woodbury, A. Freiberg, J. Phys. Chem. B 104 (2000) 9769.
- [14] M.H.C. Koolhaas, G. van der Zwan, R. van Grondelle, J. Phys. Chem. B 104 (2000) 4489.
- [15] V. Nagarjan, E.T. Johnson, J.C. Williams, W.W. Parson, J. Phys. Chem. B 103 (1999) 2297.
- [16] B.P. Krueger, G.D. Scholes, G.R. Fleming, J. Phys. Chem. B 102 (1998) 5378.
- [17] T. Meier, V. Chernyak, S. Mukamel, J. Chem. Phys. 107 (1997) 8759.
- [18] R. Monshouwer, A. Baltuška, F. van Mourik, R. van Grondelle, J. Phys. Chem. A 102 (1998) 4360.

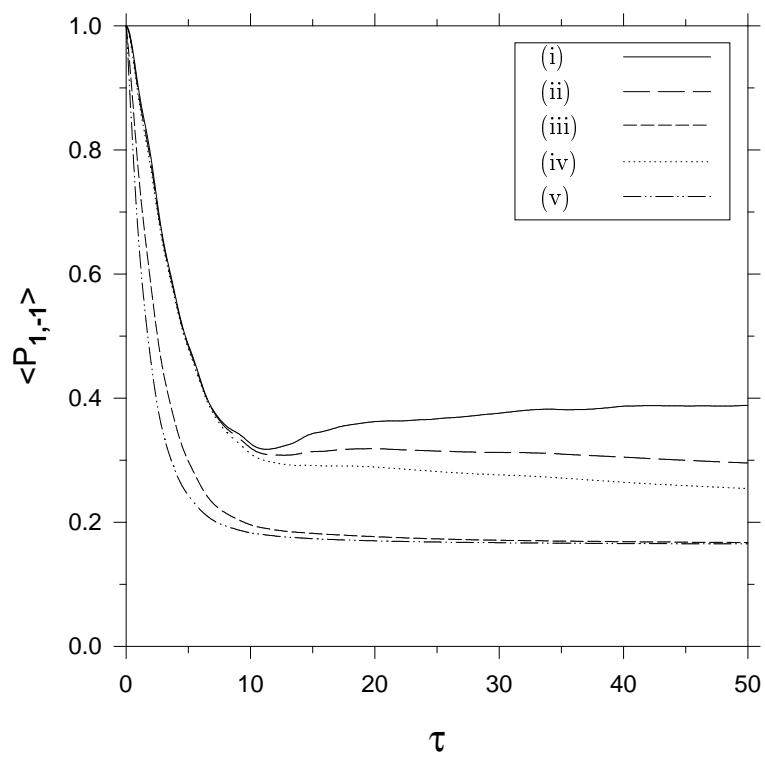
- [19] V.I. Novoderezhkin, R. Monshouwer, R. van Grondelle, *Biophysical J.* 77 (1999) 666.
- [20] V.I. Novoderezhkin, R. Monshouwer, R. van Grondelle, *J. Phys. Chem. B* 104 (2000) 12056.
- [21] V. Nagarjan, R.G. Alden, J.C. Williams, W.W. Parson, *Proc. Natl. Acad. Sci. USA* 93 (1996) 13774.
- [22] V. Nagarjan, W.W. Parson, *Biochemistry* 36 (1997) 2300.
- [23] V. Nagarjan, W.W. Parson, *J. Phys. Chem. B* 104 (2000) 4010.
- [24] R. Kumble, R. Hochstrasser, *J. Chem. Phys.* 109 (1998) 855.
- [25] O. Kühn, W. Sundström, *J. Chem. Phys.* 107 (1997) 4154
- [26] X. Hu, T. Ritz, A. Damjanovic, K. Schulten, *J. Phys. Chem. B* 101 (1997) 3854.
- [27] S.H. Lin, R. Alden, R. Islampour, H. Ma, A.A. Villaeys, *Density matrix method and femtosecond processes* (World Scientific, Singapore 1991).
- [28] A.G. Redfield, *IBM J. Res. Dev.* 1 (1957) 19.
- [29] A.G. Redfield, *Adv. Magn. Reson.* 1 (1965) 1.
- [30] V. Čápek, P. Heřman, I. Barvák, *J. Lum.* 83-84 (1999) 105.
- [31] D. Egorova, A. Köhl, W. Domcke, *Chem. Phys.* (in press).
- [32] U. Weiss, *Quantum Dissipative Systems*, 2nd ed. (World Scientific, Singapore, 1999).
- [33] N. Makri, *J. Phys. Chem. A* 102 (1998) 4414.
- [34] W.B. Davis, M.R. Wasielewski, R. Kosloff, M.A. Ratner, *J. Phys. Chem. A* 102 (1998) 9360.
- [35] R. Kosloff, M.A. Ratner, W.W. Davis, *J. Chem. Phys.* 106 (1997) 7036.
- [36] D. Kohen, C.C. Marston, D.J. Tannor, *J. Chem. Phys.* 107 (1997) 5236.
- [37] K. Blum, *Density Matrix Theory and Applications*, 2nd ed., (Plenum Press New York, 1996).
- [38] P. Reineker, in *Exciton Dynamics in Molecular Crystals and Aggregates*, Höhler, G., Ed., (Springer, Berlin, 1982).
- [39] M. Grover, R. Silbey, *J. Chem. Phys.* 54 (1971) 4843.
- [40] V. Čápek, I. Barvák, *Phys. Rev. A* 46 (1992) 7431.

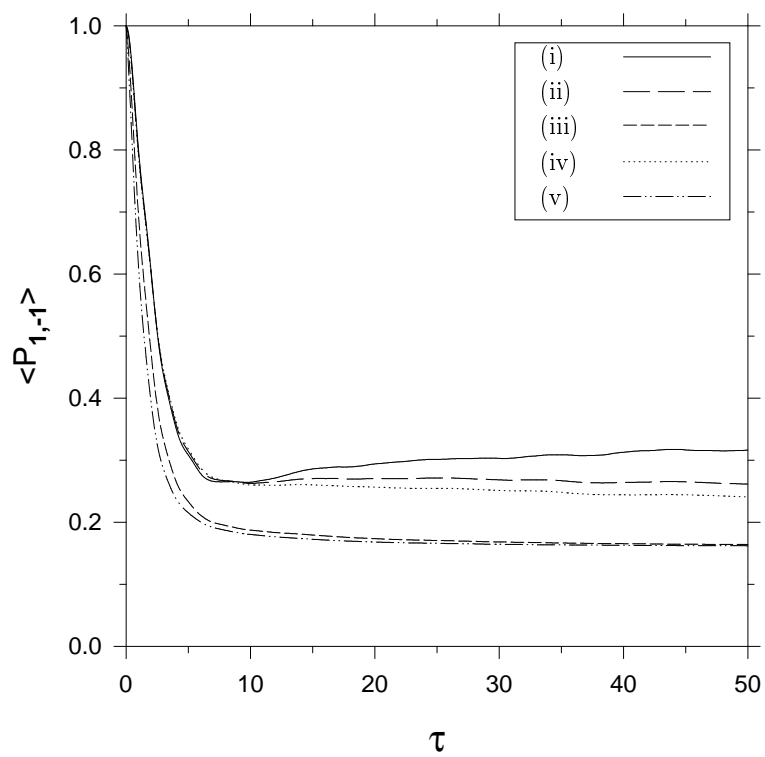
- [41] J. A. Leegwater, J. Phys. Chem. B 100 (1996) 14403.
- [42] I. Barvák, in *Large Scale Molecular Systems*, NATO ASI Series B: Physics Vol. 258, eds. W. Gans, A. Blumen, A. Aman, (Plenum Press, New York, 1991) p. 371.
- [43] I. Barvák, in *Dynamical Processes in Condensed Molecular Systems*, ed. A. Blumen, (World Scientific, Singapore, 1991) p. 275.
- [44] P. Heřman, I. Barvák, Czech. J. Phys. 48 (1998) 423.
- [45] V. May, O. Kühn, *Charge and Energy Transfer in Molecular Systems*, Wiley-WCH, Berlin (2000).
- [46] U. Kleinekathöfer, I. Kondov, M. Schreiber, Chem. Phys. (in press).
- [47] I. Kondov, U. Kleinekathöfer, M. Schreiber, J. Chem. Phys. 114 (2001) 1497.
- [48] V. Čápek, Physica A 203 (1994) 495 and 520.
- [49] V. Čápek, J. Peřina Jr., Physica A 215 (1995) 209.
- [50] V. Čápek, Z. Phys. B 99 (1996) 261.
- [51] M. Chachisvilis, O. Kühn, T. Pullerits, V. Sündstrom, J. Phys. Chem. B 101 (1997) 7275.
- [52] I. Barvák, Ch. Warns, P. Reineker, Chem. Phys. (submitted).
- [53] I. Barvák, J. Macek, J. Chin. Chem. Soc. 47 (2000) 647.
- [54] A.M. van Oijen, M. Ketelaars, J. Köhler, T.J. Aartsma, J. Schmidt, Science 285 (1999) 400.
- [55] M.V. Mostovoy, J. Knoester, J. Phys. Chem. B 104 (2000) 12355.

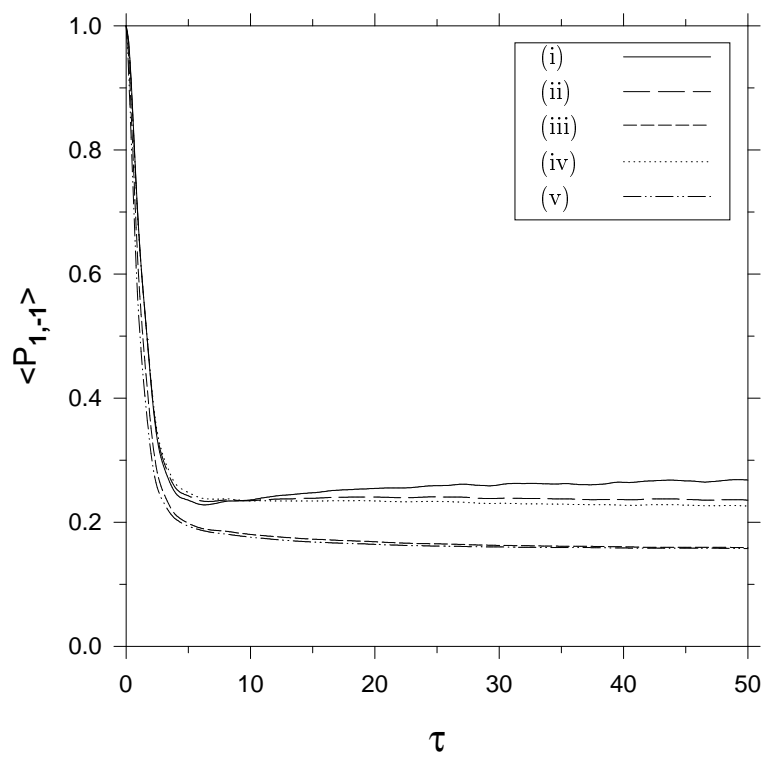


## Figure captions:

Fig. 1: Time dependence of the occupation probability  $\langle P_{\pm 1} \rangle$  for static disorder  $\Delta = 0.4$  (a),  $\Delta = 0.6$  (b),  $\Delta = 0.8$  (c) and  $\Delta = 1.0$  (d). The influence of the dynamic disorder is displayed by curves for low (ii), (iv) and room (iii), (v) temperature for  $j_0 = 0.2$  (ii), (iii), and  $j_0 = 0.4$  (iv), (v) compared to  $j_0 = 0.0$  (i).







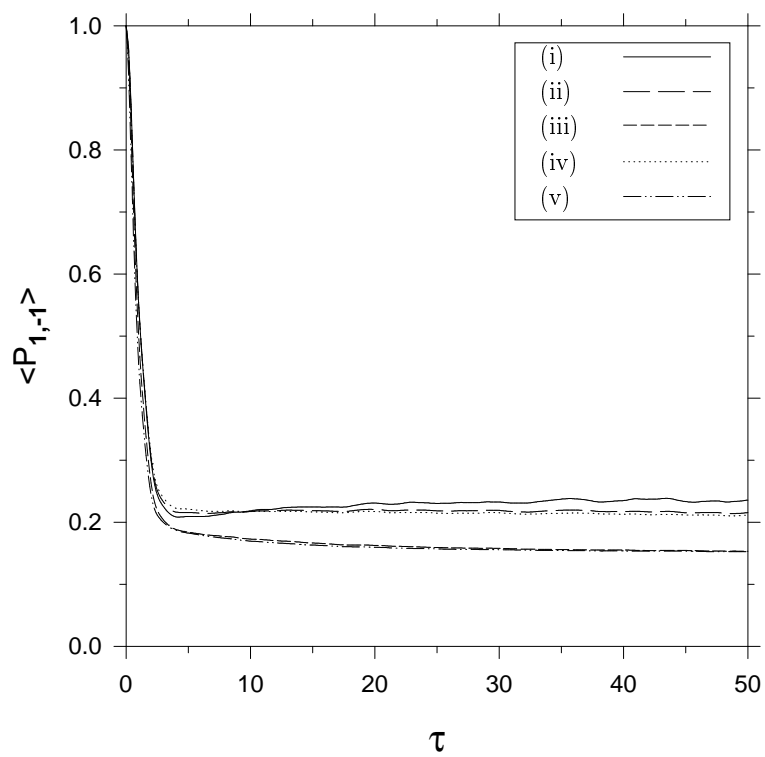


Fig. 2: Same as in Fig. 1 but for the anisotropy  $r(t)$ .

